MicroBooNE and the ν_e Interpretation of the MiniBooNE Low-Energy Excess

C. A. Argüelles,[1] I. Esteban,[2, 3] M. Hostert,[4, 5, 6] K. J. Kelly,[7] J. Kopp,[7, 8]
P. A. N. Machado,[9] I. Martinez-Soler,[1] and Y. F. Perez-Gonzalez[10]

[1]*Department of Physics & Laboratory for Particle Physics and Cosmology,*
Harvard University, Cambridge, MA 02138, USA
[2]*Center for Cosmology and AstroParticle Physics (CCAPP),*
Ohio State University, Columbus, Ohio 43210, USA
[3]*Department of Physics, Ohio State University, Columbus, Ohio 43210, USA*
[4]*Perimeter Institute for Theoretical Physics, Waterloo, ON N2J 2W9, Canada*
[5]*School of Physics and Astronomy, University of Minnesota, Minneapolis, MN 55455, USA*
[6]*William I. Fine Theoretical Physics Institute, School of Physics and Astronomy,*
University of Minnesota, Minneapolis, MN 55455, USA
[7]*Theoretical Physics Department, CERN, Esplande des Particules, 1211 Geneva 23, Switzerland*
[8]*PRISMA+ Cluster of Excellence & Mainz Institute for Theoretical Physics, Staudingerweg 7, 55128 Mainz, Germany*
[9]*Particle Theory Department, Fermi National Accelerator Laboratory, Batavia, IL 60510, USA*
[10]*Institute for Particle Physics Phenomenology, Durham University, South Road, Durham, United Kingdom*
(Dated: November 22, 2021)

A new generation of neutrino experiments is testing the 4.7σ anomalous excess of electron-like events observed in MiniBooNE. This is of huge importance for particle physics, astrophysics, and cosmology, not only because of the potential discovery of physics beyond the Standard Model, but also because the lessons we will learn about neutrino–nucleus interactions will be crucial for the worldwide neutrino program. MicroBooNE has recently released results that appear to disfavor several explanations of the MiniBooNE anomaly. Here, we show quantitatively that MicroBooNE results, while a promising start, unquestionably do not probe the full parameter space of sterile neutrino models hinted at by MiniBooNE and other data, nor do they probe the ν_e interpretation of the MiniBooNE excess in a model-independent way.

Introduction. — A specter is haunting neutrino physics: the specter of sterile neutrinos. Over the past few decades, their existence has been postulated to explain various persistent anomalies in neutrino experiments [1], in particular the excess of electron-neutrino events in the LSND [2] experiment and the excess of electron-like events in the MiniBooNE [3] experiment. If real, sterile neutrinos would bring about a profound revolution to our understanding of early-universe cosmology [4], modify neutrino emission from astrophysical sources [5–7], and dethrone the Standard Model of particle physics. Precision measurements in particle physics, cosmology, and astrophysics will remain ambiguous until we clarify whether such sterile neutrinos exist.

Recently, the MicroBooNE collaboration has released results scrutinizing the MiniBooNE anomaly, also known as the MiniBooNE low-energy excess (MBLEE). As the MicroBooNE detector is exposed to the same neutrino beam as MiniBooNE but has superior event reconstruction capabilities, it is able to differentiate between different interpretations of the MBLEE. A first MicroBooNE analysis disfavors that the MBLEE is due to underestimated production of Δ baryons followed by decays to photons at a significance of 94.8% C.L. [8].

Following that, three distinct and complementary analyses have been released, addressing whether the MBLEE is caused by an excess of electron-neutrinos in the beam [9–12]. These compare the MicroBooNE data to a signal template defined by the assumption that the ex-

pected spectrum of the ν_e excess in MiniBooNE matches exactly the difference between the data and the best-fit background prediction. Assuming this nominal template, the collaboration concludes that "the results are found to be consistent with the nominal ν_e rate expectations from the Booster Neutrino Beam and no excess of ν_e events is observed" [9]. However, as we will show, this approach is not sufficient to exclude the ν_e interpretation of the MBLEE in a model-independent way or even to exclude the sterile neutrino solution of the MBLEE. This is an important question that can have an impact on the future of the short-baseline neutrino program, as well as on a variety of alternative models [13–18] proposed to explain the MiniBooNE and LSND results.

Previous attempts to constrain the LSND and Mini-BooNE excesses suffered from insufficient sensitivity to cover the allowed parameter space [19–23]. It is essential to quantify the power of MicroBooNE as we search for definitive answers to this 20-year-old puzzle. This is the goal of this letter. We first analyze the constraints of MicroBooNE's latest results on ν_e appearance in Mini-BooNE in a more model-independent way, and then we narrow down the question to the sterile neutrino scenario.

For the first stage, we follow the procedure adopted by MicroBooNE: starting from a MiniBooNE event spectrum, we translate it into an expected excess of events in MicroBooNE, and we perform a statistical analysis of the data. After verifying that we reproduce Micro-BooNE's results when using the nominal template, we re-

peat the analysis with a set of alternative templates that are equally successful at explaining the MBLEE. These alternative templates are allowed mostly due to the systematic uncertainties on the backgrounds. As they dominate the significance of the MBLEE, we find that they change the interpretation of the MicroBooNE results significantly.

For the second stage, we perform a fit of MicroBooNE data to a simple light sterile neutrino model. We assume both a simplified oscillation scenario with only $\nu_\mu \to \nu_e$ appearance, as well as a fully-consistent oscillation model that accounts for oscillations in the MicroBooNE control samples and backgrounds.

Experimental Analysis.— To quantify the disagreement between MicroBooNE data and a ν_e interpretation of the MBLEE, we proceed as follows. All our analyses start with a hypothesis for the MBLEE. [1] The next step is the unfolding procedure, which generates an MBLEE template *before* detector effects. We apply the D'Agostini iterative method [25, 26], and we have checked upon inverting the unfolding procedure we recover the original spectrum before detector effects. To obtain the expected spectrum at MicroBooNE, we rescale the unfolded spectrum to account for the differences in exposure and detector mass between MiniBooNE and MicroBooNE [9]. We then smear the events according to MicroBooNE's energy resolution [10, 11]. To infer MicroBooNE's energy-dependent ν_e detection efficiency, we apply all previous steps to the intrinsic ν_e background, and we choose the efficiency in each reconstructed energy bin such that our results match the official MicroBooNE background prediction [10, 11]. We have checked that our efficiencies are consistent with the energy-averaged efficiencies quoted in Refs. [10, 11], and that they generate an MBLEE prediction that matches the official MicroBooNE result.

For the statistical procedure, we focus on the Charged-Current (CC) Inclusive [10] and Charged-Current Quasielastic (CCQE) [11] channels, as they comprise the leading statistical power of the experiment, and we use the data releases provided by the collaboration wherever possible. For the Inclusive analysis, we have performed several statistical tests, including both Pearson-χ^2 and CNP-χ^2 [27], as well as calculating a test statistic with or without deriving a constraint using the conditional covariance matrix formalism [10]. For all tests, we find very good agreement with the results of Ref. [10]. For clarity, in what follows we perform all statistical tests using the CNP-χ^2 formalism with the full $(137, 137)$ covariance matrix of Ref. [10]. For the CCQE analysis, in turn, we use a Poisson likelihood, where the expectation in each bin is treated as a nuisance parameter that is constrained by the covariance matrix. Our

test statistic in this latter analysis is then determined by profiling over these nuisance parameters.

Template results.— Our first approach assesses whether MicroBooNE generically rules out a ν_e interpretation of the MBLEE. In particular, the MiniBooNE backgrounds have large, correlated systematic uncertainties. These allow for different shapes of the MBLEE, that could affect the prediction at MicroBooNE.

First, we generate a set of LEE templates using a Markov-Chain Monte-Carlo (MCMC) [28] by independently re-scaling the normalization of the MiniBooNE backgrounds. [2] We group backgrounds in four classes: all intrinsic ν_e, mis-identified π^0, $\Delta \to \gamma$, and all others. To estimate how well each template fits the MiniBooNE data, we calculate its goodness-of-fit p-value using a χ^2 test statistic with the official MiniBooNE covariance matrix [29]. We follow the prescription of the MiniBooNE collaboration, that the test-statistic follows a χ^2 distribution with 8.7 degrees of freedom (while our template model has 4 degrees of freedom). This generates a set of MBLEE templates compatible with MiniBooNE data. We will refer to this analysis as the template analysis.

Figure 1 exemplifies the impact of our procedure. We show three different templates for MiniBooNE (upper panel) and the corresponding predicted excess events at MicroBooNE (lower panel): the nominal template given by the difference between the observed data and the best-fit background estimate (black); a template with significantly more events at low energies but a p-value of 87% (blue); a template with fewer events and a p-value of 87% (red); and a template corresponding to the best-fit $\nu_\mu \to \nu_e$ two-neutrino oscillation framework assuming $\Delta m^2 = 0.041$ eV^2 and $\sin^2 2\theta = 0.92$, which has a p-value of 20% (red).

The systematic uncertainties in the MiniBooNE background allow for very different shapes and rates of the MBLEE (including those coming from the sterile neutrino hypothesis) to provide a good fit to the data. These generate different predictions at MicroBooNE that will be excluded with different statistical significance. As we will show, this is crucial in constraining the interpretation of the MBLEE in terms of ν_e events at MicroBooNE.

Let us now turn to the results of our template analysis. For concreteness, for the template analysis we focus on the Inclusive analysis, which provides the best constraints on the ν_e interpretation of the MBLEE. We organize the templates in three categories by decreasing goodness-of-fit, $p > 80\%$, 10%, and 1%, and classify them by their signal strength, defined as $N/N_{\rm LEE}$ with N the number of excess events that the template predicts at MiniBooNE, and $N_{\rm LEE} = 360$ the number of excess events.

---

[1] To directly compare with MicroBooNE results, we base our analysis on the 2018 MiniBooNE data [24].

---

[2] Alternatively, we have also generated templates by independently varying the excess events in each bin. Both approaches produce consistent results.
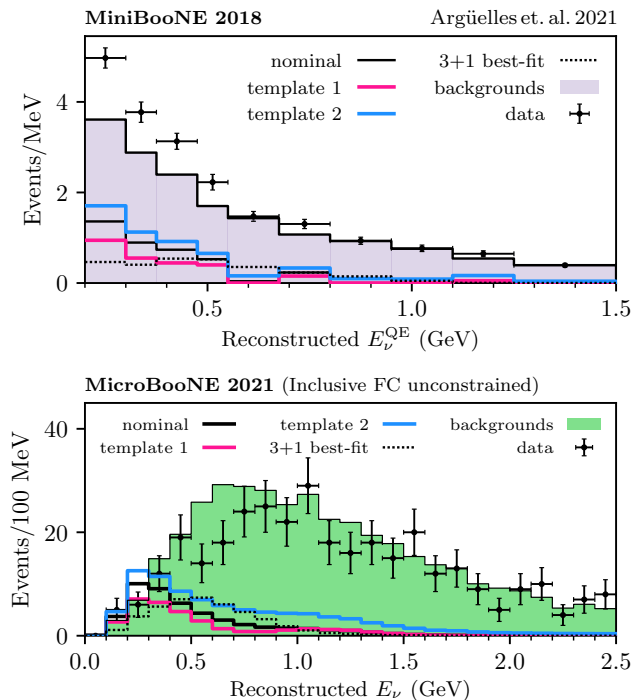
FIG. 1. The event rate at MiniBooNE (top) and Micro-BooNE (bottom) in reconstructed neutrino energy. We show several MiniBooNE templates, including that of the 3+1 oscillation best-fit, as non-stacked histograms. For MicroBooNE we show the predictions based on our unfolding procedure together with the data and unconstrained background to fully contained events.

Figure 2 shows the result of the template analysis. Each point corresponds to a different template with a well-defined signal strength and $\Delta\chi^2_{\mu B}$. To indicate the proximity to the best-fit MiniBooNE template, the points are colored by the three goodness-of-fit categories defined above. For each template, we compute the corresponding MicroBooNE $\chi^2_{\mu B}$, and construct the difference with respect to the no-excess hypothesis, $\Delta\chi^2_{\mu B}$. We also show as a black line the result of profiling over all templates with the same signal strength. The horizontal lines then correspond to the MicroBooNE 1-, 2-, 3-, and 4-σ exclusion limits [30, 31].

As we can see in Fig. 2, the introduction of shape and normalization uncertainties in the MBLEE template can either enhance or mitigate MicroBooNE's sensitivity. To illustrate the variability of the template shapes and normalization, we have marked with a star the two templates shown in Fig. 1, corresponding to two extreme points in the $p > 80\%$ region.

Nevertheless, several templates that are a good fit to MiniBooNE data cannot be excluded by MicroBooNE. In particular, we observe a large density of templates with good fits to MiniBooNE data, $p > 80\%$ (10%), well below the $\Delta\chi^2_{\mu B} = 9$ (4) line. We thus conclude that, while recent MicroBooNE results indeed constrain the
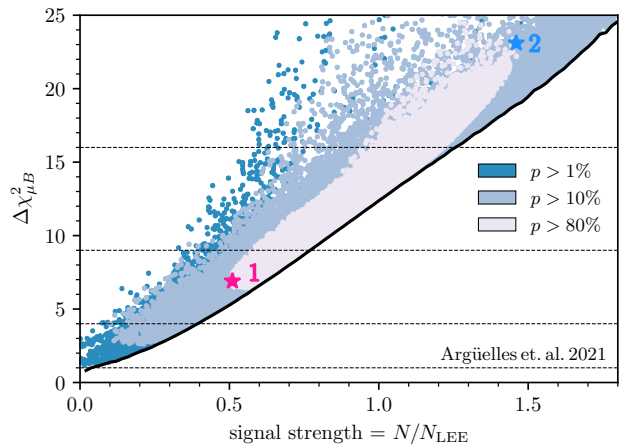

FIG. 2. The $\Delta\chi^2$ of the Inclusive ν_eCC analysis at Micro-BooNE for various templates found by our MCMC. Each point corresponds to a specific template that provides a good fit to MiniBooNE data with a p-value greater than 80%, 10%, and 1%. Horizontal lines correspond to $\Delta\chi^2_{\mu B} = 1, 4, 9, 16$. The stars correspond to templates 1 and 2 presented in Fig. 1.

ν_e interpretation of the MiniBooNE excess in a model-independent way, they do not completely rule it out.

Sterile Neutrino Analysis. — The analysis above does not rely on any particular particle physics model. As an example of a specific physics model that can explain the MBLEE, we now turn to light sterile neutrinos. They provide a simple scenario that could lead to $\nu_\mu \to \nu_e$ transitions at short baselines and have been extensively studied in the literature [1, 4, 32–34].

To perform analyses including sterile neutrinos, we use Ref. [35] and first calculate, as a function of oscillation parameters, the expected excess spectrum in MiniBooNE. Using the same procedure discussed above, we map these spectra into the expected excesses in MicroBooNE's Inclusive and CCQE analyses. We note that the efficiencies for MiniBooNE and MicroBooNE CCQE analyses decrease at large energies, while in the Inclusive Micro-BooNE analysis they stay constant.

Leveraging the data released coincident with Refs. [10, 11], we can also account for oscillations of the ν_μ and ν_e CC background expectations [3] in MicroBooNE's analyses to allow for a complete, four-neutrino oscillation analysis.

We start by discussing the results of the simplified sterile neutrino model, which assumes the backgrounds to be independent of the sterile neutrino parameters. This

---

[3] More concretely, we use the data releases provided along with Ref. [10] to determine the expected $\nu_{\mu,e}$ CC fully- and partially-contained spectra as a function of *true* neutrino energy. Oscillations are included with respect to true energy, then the distributions are mapped into *reconstructed* neutrino energy (again, using Ref. [10]) where test statistics are calculated.
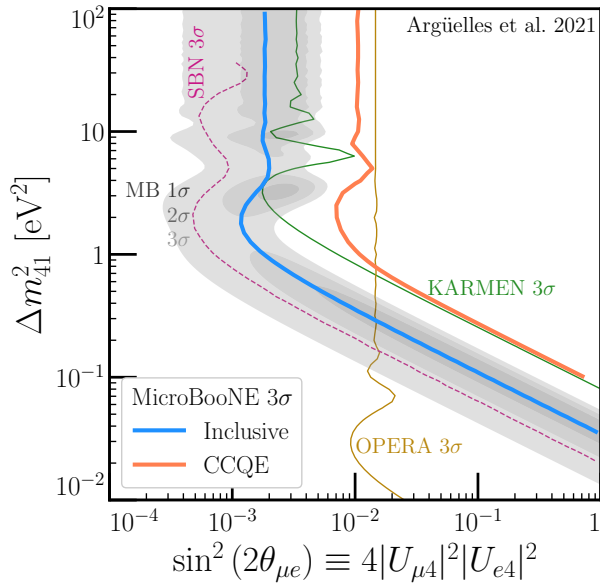
FIG. 3. MicroBooNE constraints on the sterile neutrino parameter space at 3σ C.L. (blue, inclusive and orange, CCQE). For reference, we show the MiniBooNE 1-, 2-, and 3-σ preferred regions in shades of grey [24], the future sensitivity of the three SBN detectors (pink [36]), and existing constraints from KARMEN (green [19]) and OPERA (gold [37]).

simplified model is parametrized by a squared-mass difference Δm_{41}^2 and an effective mixing angle $\sin^2 2\theta_{\mu e} \equiv 4|U_{e4}U_{\mu4}|^2$ with U the leptonic mixing matrix. Figure 3 presents the results of our analyses of MicroBooNE's inclusive and CCQE channels in blue and orange, respectively, at 3σ C.L.

While MicroBooNE data disfavors part of the region preferred by MiniBooNE, we find that there is still a large viable fraction of the parameter space, even within the 1σ preferred region of MiniBooNE. We find it unlikely that future MicroBooNE results will significantly improve on this, even though MicroBooNE has only analyzed about half of their data set, because of a deficit in their Inclusive data that generates more sensitivity than expected (*c.f.* Fig. 1, this could be due to an underfluctuation in the data or to background mismodelling). This highlights the importance of searching for sterile neutrinos with the three SBN detectors — SBND, MicroBooNE, and ICARUS — which will probe the full 2σ region preferred by MiniBooNE with less dependence on the neutrino cross section and flux.

Finally, we stress that a fully-consistent four-neutrino analysis should also consider oscillations of the backgrounds. This is relevant at MiniBooNE [16, 38], and even more for the MicroBooNE Inclusive analysis: while the former has large non-neutrino induced backgrounds, the dominant background in the latter is beam-ν_e contamination. Moreover, since other neutrino samples (particularly CC ν_μ) are used to constrain systematics and
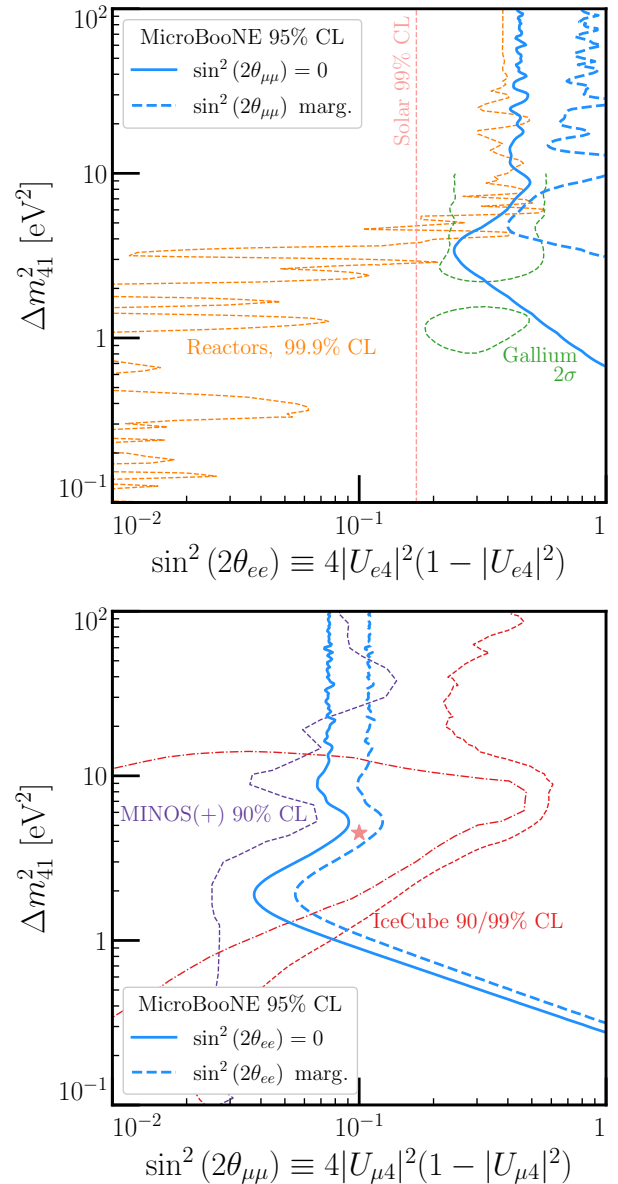

FIG. 4. MicroBoone constraints in the planes Δm_{41}^2 versus $\sin^2(2\theta_{ee})$ (left) and $\sin^2(2\theta_{\mu\mu})$ (right). In each of these panels, we have either fixed (solid lines) or profiled over (dashed) the unseen mixing angle. For comparison, we show existing constraints and preferred regions (see Refs. [39–53]).

backgrounds, oscillations should also be considered for these samples. In this regard, the CCQE analysis is complementary and distinct from the Inclusive one, as it focuses on lower neutrino energies where the neutrino contribution to the background is small. To first order, the CCQE analysis performs an appearance search, while the Inclusive simultaneously searches for appearance and disappearance.

Figure 4 presents our results in a consistent four-neutrino approach, considering oscillations of all ν_e and ν_μ samples. We show the MicroBooNE-Inclusive con-

straints in the planes Δm_{41}^2 *vs.* $\sin^2(2\theta_{ee}) \equiv 4|U_{e4}|^2(1 - |U_{e4}|)^2$ (left panel) and $\sin^2(2\theta_{\mu\mu}) \equiv 4|U_{\mu4}|^2(1 - |U_{\mu4}|)^2$ (right panel). As one can see, even in the absence of neutrino appearance, *i.e.*, U_{e4} or $U_{\mu4}$ equal zero, Micro-BooNE can still set a limit on neutrino disappearance. For muon neutrinos, the disappearance sensitivity comes from the large ν_μ data sample. For electron neutrinos, on the other hand, the sensitivity derives from the large ν_e background.

In the two panels of Fig. 4 we perform two analyses (both in blue): solid lines present the sensitivity on a mixing angle when the other is fixed to zero, whereas the dashed lines present the sensitivity when the other mixing angle has been profiled over. The disappearance prospects for ν_e are compared against hints of sterile neutrinos in Gallium experiments [39–43] and constraints from solar [44], and reactor antineutrino [45–51] experiments. The bottom panel, showing MicroBooNE ν_μ disappearance constraints, is contrasted against constraints from MINOS/MINOS+ [52] and results from Ice-Cube [53], including a 90% C.L. preferred region and best-fit point.

As one final remark on the importance of the complete four-neutrino analysis, Fig. 5 shows the constraints from MicroBooNE-Inclusive as a function of $\sin^2(2\theta_{\mu e})$ after profiling over $\sin^2(2\theta_{\mu\mu})$ in comparison with preferred regions of MiniBooNE under the same set of assumptions [54]. Even more than in Fig. 3, we see that allowed MiniBooNE parameter space persists despite the MicroBooNE-Inclusive constraints.

Our results emphasize that, while the signal-oscillation only analysis is simple and intuitive, accounting for oscillations in *all* samples is the only fully-consistent approach and can affect the interpretation of the results. This will be even more relevant for the full SBN program, particularly due to different oscillation effects among the three detectors as well as due to the increased analysis sensitivity — we *strongly* advocate for the adoption of this standard moving forward with short-baseline searches for anomalous neutrino (dis)appearance.

In this complete picture, we find results consistent with no oscillations, with a best-fit point at $\Delta m_{41}^2 = 1.38$ eV^2, $\sin^2(2\theta_{ee}) = 0.2$, $\sin^2(2\theta_{\mu\mu}) = 0$ with a significance of 0.95σ. Our results do not agree with Ref. [55]. We believe that this stems from the treatment of systematic uncertainties, as we consider correlated systematics by using the official MicroBooNE covariance matrix; and due to the fact that we account for oscillations in the partially-contained ν_e sample, which is used to obtain the constrained fully-contained ν_e sample. We also implement oscillations as a function of true neutrino energy.

Conclusions.— Does MicroBooNE rule out the ν_e interpretation of the MiniBooNE low-energy excess? And does it disfavor the sterile neutrino explanation of the excess? While current MicroBooNE analyses give us invalu-
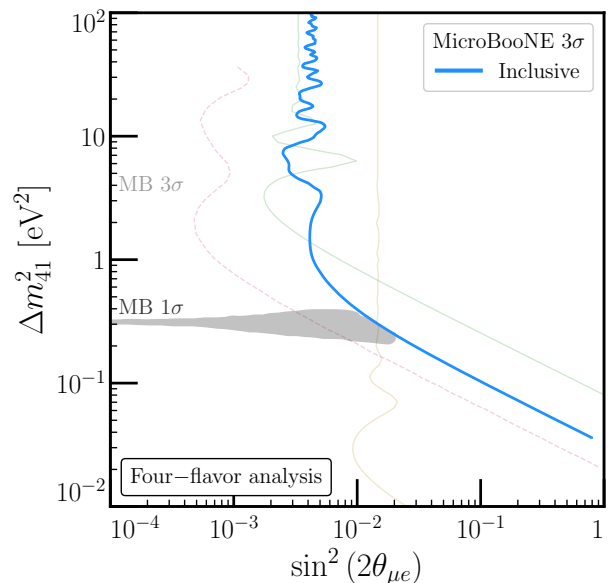

FIG. 5. MicroBooNE constraint as a function of Δm_{41}^2 and $\sin^2(2\theta_{\mu e})$ after profiling over the unseen mixing angle in a consistent four-neutrino analysis. Preferred MiniBooNE regions [54] are shown in grey. Other constraints/projections, faded for clarity, are identical to those in Fig. 3.

able insights on the MiniBooNE anomaly, we find that they still do not provide definitive answers to either of these two questions. Uncertainties on MiniBooNE backgrounds significantly impact MicroBooNE's reach, and consequently, the MiniBooNE puzzle remains wide open. To demonstrate this quantitatively, we have developed a model-independent analysis and have carried out a fully-consistent sterile neutrino fit of MicroBooNE data in the context of the MiniBooNE excess. In the first analysis, we find MiniBooNE excess templates with goodness-of-fit better than 10% that are allowed by MicroBooNE data at $< 2\sigma$. In the sterile neutrino analysis, we find that MicroBooNE's 3σ exclusion does not cover the entire 1σ preferred region by MiniBooNE.

Our findings highlight the importance of running the full SBN program, and of complementing it with the worldwide efforts to search for light sterile neutrinos in reactor [56–60], radioactive source [39], accelerator [61–64], solar [44, 65], and atmospheric neutrino [53, 66–70] experiments. Together, these experiments will have sufficient sensitivity to answer this decades-old puzzle once and for all.

————————

[1] K. N. Abazajian *et al.*, "Light Sterile Neutrinos: A White Paper," (2012), arXiv:1204.5379 [hep-ph].

[2] A. Aguilar-Arevalo *et al.* (LSND), "Evidence for neutrino oscillations from the observation of $\bar{\nu}_e$ appearance in a $\bar{\nu}_\mu$ beam," Phys. Rev. D **64**, 112007 (2001), arXiv:hep-ex/0104049.

[3] A. A. Aguilar-Arevalo *et al.* (MiniBooNE), "Updated MiniBooNE neutrino oscillation results with increased data and new background studies," Phys. Rev. D **103**, 052002 (2021), arXiv:2006.16883 [hep-ex].

[4] Basudeb Dasgupta and Joachim Kopp, "Sterile Neutrinos," Phys. Rept. **928**, 63 (2021), arXiv:2106.05913 [hep-ph].

[5] Carlos A. Argüelles, Kareem Farrag, Teppei Katori, Rishabh Khandelwal, Shivesh Mandalia, and Jordi Salvado, "Sterile neutrinos in astrophysical neutrino flavor," JCAP **02**, 015 (2020), arXiv:1909.05341 [hep-ph].

[6] Damiano F. G. Fiorillo, Gennaro Miele, Stefano Morisi, and Ninetta Saviano, "Cosmogenic neutrino fluxes under the effect of active-sterile secret interactions," Phys. Rev. D **101**, 083024 (2020), arXiv:2002.10125 [hep-ph].

[7] Damiano F. G. Fiorillo, Stefano Morisi, Gennaro Miele, and Ninetta Saviano, "Observable features in ultrahigh energy neutrinos due to active-sterile secret interactions," Phys. Rev. D **102**, 083014 (2020), arXiv:2007.07866 [hep-ph].

[8] P. Abratenko *et al.* (MicroBooNE), "Search for Neutrino-Induced Neutral Current Δ Radiative Decay in MicroBooNE and a First Test of the MiniBooNE Low Energy Excess Under a Single-Photon Hypothesis," (2021), arXiv:2110.00409 [hep-ex].

[9] P. Abratenko *et al.* (MicroBooNE), "Search for an Excess of Electron Neutrino Interactions in MicroBooNE Using Multiple Final State Topologies," (2021), arXiv:2110.14054 [hep-ex].

[10] P. Abratenko *et al.* (MicroBooNE), "Search for an anomalous excess of inclusive charged-current ν_e interactions in the MicroBooNE experiment using Wire-Cell reconstruction," (2021), arXiv:2110.13978 [hep-ex].

[11] P. Abratenko *et al.* (MicroBooNE), "Search for an anomalous excess of charged-current quasi-elastic ν_e interactions with the MicroBooNE experiment using Deep-Learning-based reconstruction," (2021), arXiv:2110.14080 [hep-ex].

[12] P. Abratenko *et al.* (MicroBooNE), "Search for an anomalous excess of charged-current ν_e interactions without pions in the final state with the MicroBooNE experiment," (2021), arXiv:2110.14065 [hep-ex].

[13] Sergio Palomares-Ruiz, Silvia Pascoli, and Thomas Schwetz, "Explaining LSND by a decaying sterile neutrino," JHEP **09**, 048 (2005), arXiv:hep-ph/0505216 [hep-ph].

[14] Yang Bai, Ran Lu, Sida Lu, Jordi Salvado, and Ben A. Stefanek, "Three Twin Neutrinos: Evidence from LSND and MiniBooNE," Phys. Rev. **D93**, 073004 (2016), arXiv:1512.05357 [hep-ph].

[15] Zander Moss, Marjon H. Moulai, Carlos A. Argüelles, and Janet M. Conrad, "Exploring a nonminimal sterile neutrino model involving decay at IceCube," Phys. Rev. **D97**, 055017 (2018), arXiv:1711.05921 [hep-ph].

[16] Mona Dentler, Ivan Esteban, Joachim Kopp, and Pedro Machado, "Decaying Sterile Neutrinos and the Short Baseline Oscillation Anomalies," Phys. Rev. D **101**, 115013 (2020), arXiv:1911.01427 [hep-ph].

[17] André de Gouvêa, O. L. G. Peres, Suprabh Prakash, and G. V. Stenico, "On The Decaying-Sterile Neutrino Solution to the Electron (Anti)Neutrino Appearance Anomalies," JHEP **07**, 141 (2020), arXiv:1911.01447 [hep-ph].

[18] Matheus Hostert and Maxim Pospelov, "Constraints on decaying sterile neutrinos from solar antineutrinos," Phys. Rev. D **104**, 055031 (2021), arXiv:2008.11851 [hep-ph].

[19] B. Armbruster *et al.* (KARMEN), "Upper limits for neutrino oscillations muon-anti-neutrino —> electron-anti-neutrino from muon decay at rest," Phys. Rev. D **65**, 112001 (2002), arXiv:hep-ex/0203021.

[20] N. Agafonova *et al.* (OPERA), "Search for $\nu_\mu \to \nu_e$ oscillations with the OPERA experiment in the CNGS beam," JHEP **07**, 004 (2013), [Addendum: JHEP 07, 085 (2013)], arXiv:1303.3953 [hep-ex].

[21] M. Antonello *et al.* (ICARUS), "Search for anomalies in the ν_e appearance from a ν_μ beam," Eur. Phys. J. C **73**, 2599 (2013), arXiv:1307.4699 [hep-ex].

[22] P. Astier *et al.* (NOMAD), "Search for nu(mu) —> nu(e) oscillations in the NOMAD experiment," Phys. Lett. B **570**, 19–31 (2003), arXiv:hep-ex/0306037.

[23] L. Borodovsky *et al.*, "Search for muon-neutrino oscillations muon-neutrino —> electron-neutrino (anti-muon-neutrino —> anti-electron-neutrino in a wide band neutrino beam," Phys. Rev. Lett. **68**, 274–277 (1992).

[24] A. A. Aguilar-Arevalo *et al.* (MiniBooNE), "Significant Excess of ElectronLike Events in the MiniBooNE Short-Baseline Neutrino Experiment," Phys. Rev. Lett. **121**, 221801 (2018), arXiv:1805.12028 [hep-ex].

[25] G. D'Agostini, "A Multidimensional unfolding method based on Bayes' theorem," Nucl. Instrum. Meth. A **362**, 487–498 (1995).

[26] MicroBooNE Collaboration, "MicroBooNE low-energy excess signal prediction from unfolding MiniBooNE Monte-Carlo and data," MICROBOONE-NOTE-1043-PUB (2018).

[27] Xiangpan Ji, Wenqiang Gu, Xin Qian, Hanyu Wei, and Chao Zhang, "Combined Neyman–Pearson chi-square: An improved approximation to the Poisson-likelihood chi-square," Nucl. Instrum. Meth. A **961**, 163677 (2020), arXiv:1903.07185 [physics.data-an].

[28] Daniel Foreman-Mackey, David W. Hogg, Dustin Lang, and Jonathan Goodman, "emcee: The mcmc hammer," Publications of the Astronomical Society of the Pacific

125, 306–312 (2013).

[29] A. A. Aguilar-Arevalo *et al.* (MiniBooNE), "MiniBooNE Data Releases," (2021), arXiv:2110.15055 [hep-ex].

[30] S. S. Wilks, "The large-sample distribution of the likelihood ratio for testing composite hypotheses," Ann. Math. Statist. **9**, 60–62 (1938).

[31] Sara Algeri, Jelle Aalbers, Knut Dundas Morå, and Jan Conrad, "Searching for new physics with profile likelihoods: Wilks and beyond," (2019), arXiv:1911.10237 [physics.data-an].

[32] S. Gariazzo, C. Giunti, M. Laveder, Y. F. Li, and E. M. Zavanin, "Light sterile neutrinos," J. Phys. G **43**, 033001 (2016), arXiv:1507.08204 [hep-ph].

[33] A. Diaz, C. A. Argüelles, G. H. Collin, J. M. Conrad, and M. H. Shaevitz, "Where Are We With Light Sterile Neutrinos?" Phys. Rept. **884**, 1–59 (2020), arXiv:1906.00045 [hep-ex].

[34] Sebastian Böser, Christian Buck, Carlo Giunti, Julien Lesgourgues, Livia Ludhova, Susanne Mertens, Anne Schukraft, and Michael Wurm, "Status of Light Sterile Neutrino Searches," Prog. Part. Nucl. Phys. **111**, 103736 (2020), arXiv:1906.01739 [hep-ex].

[35] Mona Dentler, Álvaro Hernández-Cabezudo, Joachim Kopp, Pedro A. N. Machado, Michele Maltoni, Ivan Martinez-Soler, and Thomas Schwetz, "Updated Global Analysis of Neutrino Oscillations in the Presence of eV-Scale Sterile Neutrinos," JHEP **08**, 010 (2018), arXiv:1803.10661 [hep-ph].

[36] Pedro AN Machado, Ornella Palamara, and David W Schmitz, "The Short-Baseline Neutrino Program at Fermilab," Ann. Rev. Nucl. Part. Sci. **69**, 363–387 (2019), arXiv:1903.04608 [hep-ph].

[37] N. Agafonova *et al.* (OPERA), "Final results of the search for $\nu_\mu \to \nu_e$ oscillations with the OPERA detector in the CNGS beam," JHEP **06**, 151 (2018), arXiv:1803.11400 [hep-ex].

[38] Joachim Kopp, Pedro A. N. Machado, Michele Maltoni, and Thomas Schwetz, "Sterile Neutrino Oscillations: The Global Picture," JHEP **05**, 050 (2013), arXiv:1303.3011 [hep-ph].

[39] V. V. Barinov *et al.*, "Results from the Baksan Experiment on Sterile Transitions (BEST)," (2021), arXiv:2109.11482 [nucl-ex].

[40] J. N. Abdurashitov *et al.* (SAGE), "Measurement of the response of the Russian-American gallium experiment to neutrinos from a Cr-51 source," Phys. Rev. C **59**, 2246–2263 (1999), arXiv:hep-ph/9803418.

[41] J. N. Abdurashitov *et al.*, "Measurement of the response of a Ga solar neutrino experiment to neutrinos from an Ar-37 source," Phys. Rev. C **73**, 045805 (2006), arXiv:nucl-ex/0512041.

[42] M. Altmann *et al.* (GNO), "Complete results for five years of GNO solar neutrino observations," Phys. Lett. B **616**, 174–190 (2005), arXiv:hep-ex/0504037.

[43] F. Kaether, W. Hampel, G. Heusser, J. Kiko, and T. Kirsten, "Reanalysis of the GALLEX solar neutrino flux and source experiments," Phys. Lett. B **685**, 47–54 (2010), arXiv:1001.2731 [hep-ex].

[44] Kim Goldhagen, Michele Maltoni, Shayne Reichard, and Thomas Schwetz, "Testing sterile neutrino mixing with present and future solar neutrino data," (2021), arXiv:2109.14898 [hep-ph].

[45] Jeffrey M. Berryman and Patrick Huber, "Sterile Neutrinos and the Global Reactor Antineutrino Dataset," JHEP **01**, 167 (2021), arXiv:2005.01756 [hep-ph].

[46] Y. Declais *et al.*, "Search for neutrino oscillations at 15-meters, 40-meters, and 95-meters from a nuclear power reactor at Bugey," Nucl. Phys. B **434**, 503–534 (1995).

[47] I Alekseev *et al.* (DANSS), "Search for sterile neutrinos at the DANSS experiment," Phys. Lett. B **787**, 56–63 (2018), arXiv:1804.04046 [hep-ex].

[48] D. Adey *et al.* (Daya Bay), "Measurement of the Electron Antineutrino Oscillation with 1958 Days of Operation at Daya Bay," Phys. Rev. Lett. **121**, 241805 (2018), arXiv:1809.02261 [hep-ex].

[49] H. de Kerret *et al.* (Double Chooz), "Double Chooz θ_{13} measurement via total neutron capture detection," Nature Phys. **16**, 558–564 (2020), arXiv:1901.09445 [hep-ex].

[50] Y. J. Ko *et al.* (NEOS), "Sterile Neutrino Search at the NEOS Experiment," Phys. Rev. Lett. **118**, 121802 (2017), arXiv:1610.05134 [hep-ex].

[51] G. Bak *et al.* (RENO), "Measurement of Reactor Antineutrino Oscillation Amplitude and Frequency at RENO," Phys. Rev. Lett. **121**, 201801 (2018), arXiv:1806.00248 [hep-ex].

[52] P. Adamson *et al.* (MINOS+), "Search for sterile neutrinos in MINOS and MINOS+ using a two-detector fit," Phys. Rev. Lett. **122**, 091803 (2019), arXiv:1710.06488 [hep-ex].

[53] M. G. Aartsen *et al.* (IceCube), "eV-Scale Sterile Neutrino Search Using Eight Years of Atmospheric Muon Neutrino Data from the IceCube Neutrino Observatory," Phys. Rev. Lett. **125**, 141801 (2020), arXiv:2005.12942 [hep-ex].

[54] Vedran Brdar and Joachim Kopp, "An Altarelli Cocktail for the MiniBooNE Anomaly?" (2021), arXiv:2109.08157 [hep-ph].

[55] Peter B. Denton, "Sterile Neutrino Searches with MicroBooNE: Electron Neutrino Disappearance," (2021), arXiv:2111.05793 [hep-ph].

[56] N. Allemandou *et al.* (STEREO), "The STEREO Experiment," JINST **13**, P07009 (2018), arXiv:1804.09052 [physics.ins-det].

[57] J. Ashenfelter *et al.* (PROSPECT), "The PROSPECT Reactor Antineutrino Experiment," Nucl. Instrum. Meth. A **922**, 287–309 (2019), arXiv:1808.00097 [physics.ins-det].

[58] I. Alekseev *et al.*, "DANSS: Detector of the reactor AntiNeutrino based on Solid Scintillator," JINST **11**, P11011 (2016), arXiv:1606.02896 [physics.ins-det].

[59] A. P. Serebrov *et al.*, "Search for sterile neutrinos with the Neutrino-4 experiment and measurement results," Phys. Rev. D **104**, 032003 (2021), arXiv:2005.05301 [hep-ex].

[60] Matthieu Licciardi (Stereo), "Results of STEREO and PROSPECT, and status of sterile neutrino searches," in *55th Rencontres de Moriond on Electroweak Interactions and Unified Theories* (2021) arXiv:2105.13776 [hep-ex].

[61] S. Ajimura *et al.*, "Technical Design Report (TDR): Searching for a Sterile Neutrino at J-PARC MLF (E56, JSNS2)," (2017), arXiv:1705.08629 [physics.ins-det].

[62] Fumihiko Suekane (JSNS2), "Status of JSNS^2 experiment," PoS **NuFact2019**, 129 (2020).

[63] J. Alonso, C. A. Argüelles, J. M. Conrad, Y. D. Kim, D. Mishins, S. H. Seo, M. Shaevitz, J. Spitz, and D. Winklehner, "Neutrino Physics Opportunities with the IsoDAR Source at Yemilab," (2021), arXiv:2111.09480 [hep-ex].

[64] J. R. Alonso *et al.*, "IsoDAR@Yemilab: A Conceptual Design Report for the Deployment of the Isotope Decay-At-Rest Experiment in Korea's New Underground Laboratory, Yemilab," (2021), arXiv:2110.10635 [physics.ins-det].

[65] André de Gouvêa, Emma McGinness, Ivan Martinez-Soler, and Yuber F. Perez-Gonzalez, "*pp* Solar Neutrinos at DARWIN," (2021), arXiv:2111.02421 [hep-ph].

[66] K. Abe *et al.* (Super-Kamiokande), "Limits on sterile neutrino mixing using atmospheric neutrinos in Super-Kamiokande," Phys. Rev. D **91**, 052019 (2015), arXiv:1410.2008 [hep-ex].

[67] A. Albert *et al.* (ANTARES), "Measuring the atmospheric neutrino oscillation parameters and constraining the 3+1 neutrino model with ten years of ANTARES data," JHEP **06**, 113 (2019), arXiv:1812.08650 [hep-ex].

[68] Benjamin R. Smithers, Benjamin J. P. Jones, Carlos A. Argüelles, Janet M. Conrad, and Alejandro Diaz, "Cascade Appearance Signatures of Sterile Neutrinos at 1-100 TeV," (2021), arXiv:2111.08722 [hep-ph].

[69] Alba Domi and Joao Coelho (KM3NeT, ANTARES), "Search for Sterile Neutrinos with KM3NeT/ORCA," PoS **ICRC2019**, 870 (2021).

[70] Yabin Wang and Osamu Yasuda, "Search for sterile neutrinos by shower events at a future neutrino telescope," (2021), arXiv:2110.12655 [hep-ph].

Supplemental Material

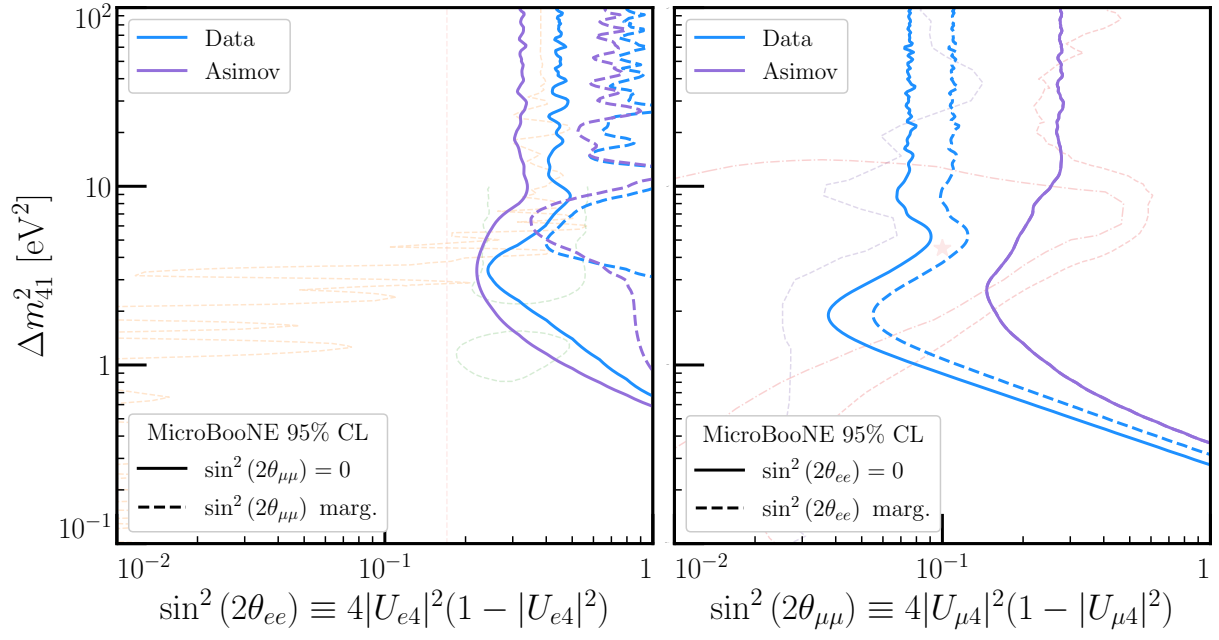## Comparison of Results to Asimov Sensitivity Expectations

In the *Sterile Neutrino Analysis* section, see Fig. 3, we presented the 3σ derived constraints on $\sin^2{(2\theta_{\mu e})}$ vs. Δm^2_{41} from the MicroBooNE Inclusive and CCQE analyses, and contrasted these constraints against existing and proposed future results. For completeness, in this appendix, we provide a comparison between the results from MicroBooNE data and the expected Asimov sensitivity, i.e., replacing the observed data with the expected background in our test statistics.
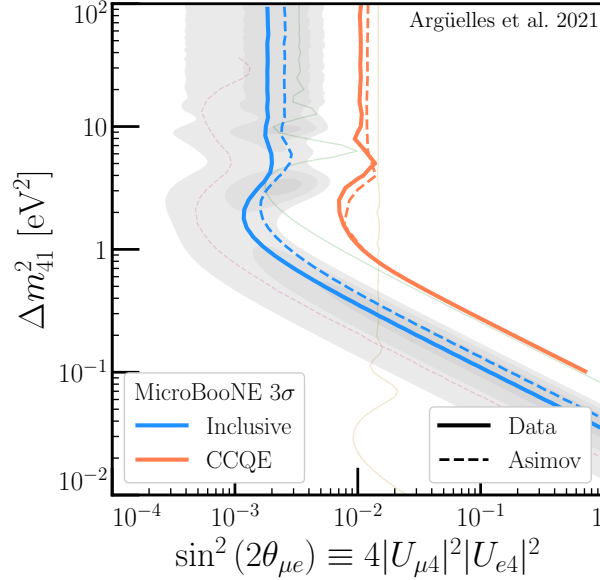
SUPPL. FIG. 1. Comparison of MicroBooNE constraints (solid lines) with the expected Asimov sensitivity (dashed) of each analysis, both at 3σ C.L. Blue lines correspond to the inclusive analysis, where orange correspond to the CCQE one. Constraints/preferred regions in this panel, dimmed for clarity, are identical to those shown and labeled in Fig. 3.

Suppl. Fig. 1 presents this comparison. As discussed in the *Template Analysis* section, the deficit of observed events relative to the expected background rate leads to a more powerful constraint than expected in both analyses, but especially so in the Inclusive one (see e.g. Fig. 1).

Suppl. Fig. 2 repeats this data/Asimov comparison for the results of Fig. 4, comparing data results in blue with Asimov expectations in purple. Here we focus, as in the main text, on the MicroBooNE Inclusive analysis. In both panels, as in Fig. 4, solid lines correspond to the analysis with the other mixing angle fixed to zero, whereas the dashed lines include profiling over the unseen angle. We see in the right panel that the data result exceeds the sensitivity greatly – this is driven by the observed ν_μ CC excess observed in both the Fully-Contained and Partially-Contained samples. These samples also modify the expectation of ν_e CC event rates due to large correlations, which has a non-negligible impact on the sensitivity to $\sin^2{(2\theta_{ee})}$ in the left panel.

SUPPL. FIG. 2. Comparison of MicroBooNE constraints (blue) with the Asimov sensitivity expectation (purple) at 95% C.L. as a function of $\sin^2(2\theta_{ee})$ and $\sin^2(2\theta_{\mu\mu})$ vs. Δm_{41}^2. Faded lines are identical to those in Fig. 4 and are only dimmed for clarity of comparison. In each panel, the solid (dashed) lines correspond to fixing (profiling over) the unseen mixing angle.